

# ERK1/2 and p38-MAPK signalling pathways, through MSK1, are involved in NF- $\kappa$ B transactivation during oxidative stress in skeletal myoblasts

Eirini Kefaloyianni, Catherine Gaitanaki, Isidoros Beis \*

*Department of Animal and Human Physiology, School of Biology, Faculty of Sciences, University of Athens, Panepistimioupolis, Athens 157 84, Greece*

Received 8 March 2006; accepted 11 May 2006  
Available online 30 June 2006

## Abstract

Skeletal muscle is highly adapted to respond to oxidative imbalances, since it is continuously subjected to an increased production of reactive oxygen species (ROS) during exercise. Oxidative stress, however, has been associated with skeletal muscle atrophy and damage in many diseases. In this study, we examined whether MAPK and NF- $\kappa$ B pathways participate in the response of skeletal myoblasts to oxidative stress, and whether there is a cross talk between these pathways. H<sub>2</sub>O<sub>2</sub> induced a strong activation of ERKs, JNKs and p38-MAPK in a time- and dose-dependent profile. ERK and JNK activation by H<sub>2</sub>O<sub>2</sub>, but not that of p38-MAPK, was mediated by Src kinase and, at least in part, by EGFR. H<sub>2</sub>O<sub>2</sub> also stimulated a mild translocation of NF- $\kappa$ B to the nucleus, as well as a moderate phosphorylation of its endogenous cytoplasmic inhibitor I $\kappa$ B (at Ser32/36), without any significant decrease in I $\kappa$ B total levels. Moreover, oxidative stress induced a strong phosphorylation of NF- $\kappa$ B p65 subunit at Ser536 and Ser276. Inhibition of MAPK pathways by selective inhibitors did not appear to affect H<sub>2</sub>O<sub>2</sub>-induced nuclear translocation of NF- $\kappa$ B or the phosphorylation of I $\kappa$ B. In contrast, phosphorylation of p65 at Ser276 was found to be mediated by MSK1, a substrate of both ERKs and p38-MAPK. In conclusion, it seems that, during oxidative stress, NF- $\kappa$ B translocation to the nucleus is most likely not related with the MAPK activation, while p65 phosphorylations are in part mediated by MAPKs pathways, probably modifying signal specificity.

© 2006 Elsevier Inc. All rights reserved.

*Keywords:* NF- $\kappa$ B; MAPK; Signal transduction; Myoblasts; MSK1; Oxidative stress

## 1. Introduction

Skeletal muscle is normally subjected to oxidative stress during exercise, since intense contractile activity is associated with an increase in free radical production [1–3]. Thus, skeletal muscle is highly adapted to respond, *in vivo*, to reduction–oxidation (redox) imbalances. Reactive oxygen species (ROS), however, may also contribute to muscle degeneration in many diseases, such as exercise-induced muscle injuries [4], as well as muscular dystrophies [5] and atrophies [6,7]. All these pathological conditions have been associated with increased markers of oxidative stress, including lipid and protein oxidation and increases in antioxidant levels [5,6,8]. Therefore, the investigation of skeletal myocytes responses to oxidative stress is of highly importance, in order to understand the physiological adaptations and to delineate the origin of muscle disorders.

In order to respond to oxidative stress, cells display adaptive mechanisms involved in increasing their antioxidant defenses. Elevated levels of ROS appear to be detected by redox sensitive regulatory molecules in the cell that can trigger various signal transduction cascades [9,10]. Among the major pathways activated during ROS accumulation, the mitogen-activated protein kinases (MAPKs) and the nuclear factor- $\kappa$ B (NF- $\kappa$ B) ones are included [11,12]. These pathways regulate the function of cytoplasmic components and the expression of a variety of genes involved either in survival and proliferation or in the induction of cell death, depending on the strength and the kind of the stimulus, as well as the cell-type examined [13–15].

MAPKs include four subfamilies, the best characterised of which are the ERKs, JNKs and p38-MAPK, and can be activated by a variety of stimuli. Every MAPK subfamily is composed of a three sequentially acting kinase module, MEKK, MEK and MAPK, each one activating the next via phosphorylation. Their substrates, located in the cytoplasm as well as in the nucleus, include other kinases, transcription factors, phospholipases and

\* Corresponding author. Tel.: +30 210 7274244; fax: +30 210 7274635.  
E-mail address: [ibeis@biol.uoa.gr](mailto:ibeis@biol.uoa.gr) (I. Beis).

cytoskeletal proteins [14,16,17]. In general, ERKs are mainly involved in anabolic processes, such as cell division, growth and differentiation, whereas JNKs and p38-MAPK are mostly associated with cellular responses to diverse stresses, such as UV irradiation and osmotic shock [13,14].

Although MAPK activation during oxidative stress has been extensively studied, the exact triggering signal of these pathways remains obscure. In previous studies, the oxidative stress-induced MAPK activation had been associated with kinases of the Src family [18,19] and various growth factor receptors such as epidermal growth factor receptor (EGFR) [20–22]. Other studies, however, implicate thioredoxin (Trx) and apoptosis signal-regulating kinase 1 (ASK1) proteins in MAPK activation [23,24]. In particular, it is known that ROS induce the dimerization of Trx and its subsequent dissociation from ASK1, resulting in the activation of the latter. Activated ASK1 can phosphorylate and activate MEK3/6 and MEK4/7, leading to the activation of p38-MAPK and JNKs, respectively [25,26]. Another important mechanism involved in the increased MAPK phosphorylation is the possible oxidative inhibition of specific protein phosphatases that regulate their function [27].

The first eukaryotic transcription factor shown to respond directly to oxidative stress was NF- $\kappa$ B [28]. Initial studies had proposed that an increase in ROS levels was essential for the NF- $\kappa$ B activation. Recent experimental data though, indicate that redox-induced activation of NF- $\kappa$ B is highly cell-type-dependent [29]. According to the classical pathway, activation of NF- $\kappa$ B, especially the most common form, p50-p65 dimer, depends on the phosphorylation of its endogenous inhibitor, I $\kappa$ B, mainly by I $\kappa$ B kinases (IKKs). This leads to ubiquitination and subsequent proteosomal degradation of I $\kappa$ B, while the liberated NF- $\kappa$ B dimer translocates to the nucleus, where it activates specific target genes [30,31].

A growing body of recent data, however, indicates that post-translational modifications of NF- $\kappa$ B, particularly phosphorylation and acetylation, play additional significant roles in the activation of the transcription factor [32–34]. Four different serine residues of p65 (RelA) subunit can be phosphorylated. Among them, Ser276 and Ser536 may be phosphorylated by the mitogen- and stress-activated kinase 1 (MSK1) [35] or the ribosomal S6 kinase 1 (RSK1) [36], respectively. Since members of the MAPK family activate these kinases, they represent a potential interaction point between these two pathways.

Although there is evidence available concerning a positive regulation of NF- $\kappa$ B by ERKs and p38-MAPK by the tumor necrosis factor- $\alpha$  (TNF- $\alpha$ ) in various cell types [37,38] or during myoblast differentiation [39], very little is known on a possible linkage between these pathways under oxidative stress in the skeletal muscle.

In the present study, we demonstrate that oxidative stress induces the activation of both, MAPK and NF- $\kappa$ B pathways in C2 skeletal myoblasts. C2 myoblasts resemble the resident in adult muscle satellite cells. Since differentiated muscle cells are unable to proliferate, myoblasts are responsible for any muscle growth or regeneration [40]; therefore, their response to oxidative stress-induced muscle degeneration is crucial. Furthermore, our studies show for the first time a cross talk between the

ERKs/MSK1, p38-MAPK/MSK1 and the NF- $\kappa$ B signalling pathways in skeletal myoblasts.

## 2. Materials and methods

### 2.1. Materials

All chemicals were of the highest grade available and purchased from Sigma-Aldrich Chemie GmbH (89552 Steinheim, Germany) and Merck (Darmstadt 64293, Germany). The enhanced chemiluminescence (ECL) kit was from Amersham International (Uppsala 751 84, Sweden). Bradford protein assay reagent was from Bio-Rad (Hercules, California 94547, USA). Nitrocellulose (0.45  $\mu$ m) was obtained from Schleicher and Schuell (Keene N.H. 03431, USA). The selective inhibitors SB203580 (#559389), PD98059 (#513000), SP600125 (#4201119), AG1478 (#658552) and PP2 (#529573) were obtained from Calbiochem-Novabiochem (La Jolla, CA, USA) and the inhibitor GW5074 (#G6416) was purchased from Sigma-Aldrich Chemie GmbH. [ $\gamma$ - $^{32}$ P]ATP was from Hartmann Analytic GmbH (Braunschweig, Germany). The NF- $\kappa$ B consensus oligonucleotide (E3292), T4 polynucleotide kinase (M4101) and T4 polynucleotide kinase buffer (C1313) were obtained from Promega (Madison, USA). Poly dI-dC (P4929) was from Sigma-Aldrich Chemie GmbH.

Antibodies specific for the phosphorylated forms of p38-MAPK (#9211), ERKs (#9101), JNKs (#9251), p65-Ser536 (#3031), p65-Ser276 (#3037), I $\kappa$ B (#9246), MSK1 (#9595), as well as for the total p38-MAPK (#9212), ERKs (#9102), JNKs (#9252) and for activated caspase-3 (#9665) were obtained from Cell Signalling Technology (Beverly, MA 01915, USA). Antibodies specific for the total p65 (#sc109) and I $\kappa$ B (#sc371) were from Santa Cruz Biotechnology Inc. (California 95060, USA). The antibody against actin (#A2103) was from Sigma-Aldrich Chemie GmbH. Prestained molecular mass markers (#P7708) were from New England Biolabs (Beverly, MA 01915, USA). Biotinylated anti-rabbit (#P0448) and anti-mouse (#P0447) antibodies were from DAKO A/S (DK-2600 Glostrup, Denmark). X-OMAT AR film (13  $\times$  18 cm) was purchased from Eastman Kodak Company (New York 14650, USA).

Cell culture supplies including fetal bovine serum (FBS #A15-043), Dulbecco's Modified Eagle's Medium (DMEM #E15-843), antibiotics (penicillin, streptomycin #P11-010) and trypsin/EDTA were purchased from PAA Laboratories GmbH, Pasching, Austria.

### 2.2. Cell cultures and treatments

In all experiments, C2 murine myoblasts were used. This cell line was a kind gift from Dr. Yaffe [41]. Cells were grown in a humidified 95% air–5% CO<sub>2</sub> atmosphere, in DMEM supplemented with 15% (v/v) heat-inactivated fetal bovine serum (FBS), 100 U/ml penicillin and 100  $\mu$ g/ml streptomycin. Experiments were carried out at a 70% confluence and after at least 3 h of serum deprivation. Exogenous H<sub>2</sub>O<sub>2</sub> was used as the oxidant at the concentrations and for the times indicated. When pharmacological inhibitors were used, they were dissolved in DMSO and added to the medium 30 min prior to treatment with H<sub>2</sub>O<sub>2</sub>.

### 2.3. Protein extraction

Cells were washed twice in ice-cold Ca<sup>2+</sup>–Mg<sup>2+</sup>-free phosphate buffer saline (PBS) and extracted in buffer G [20 mM Hepes, pH 7.5, 20 mM  $\beta$ -glycerophosphate, 20 mM NaF, 2 mM EDTA, 0.2 mM Na<sub>3</sub>VO<sub>4</sub>, 5 mM dithiothreitol (DTT), 10 mM benzamidine, 200  $\mu$ M leupeptin, 10  $\mu$ M *trans*-epoxy succinyl-L-leucylamido-(4-guanidino)butane, 300  $\mu$ M phenyl methyl sulfonyl fluoride (PMSF), 0.5% (v/v) Triton X-100] on ice, for 30 min. Samples were centrifuged (10,000 $\times$ g, 5 min, 4  $^{\circ}$ C) and the supernatants were boiled with 0.33 volumes of SDS/PAGE sample buffer (4 $\times$ ) [0.33 M Tris/HCl, pH 6.8, 10% (w/v) SDS, 13% (v/v) glycerol, 20% (v/v) 2-mercaptoethanol, 0.2% (w/v) bromophenol blue].

For the detection of caspase-3 active fragment, cells were lysed with chaps buffer [50 mM HEPES/KOH pH 6.5, 2 mM EDTA, 0.1% (w/v) chaps, 20  $\mu$ g/ml leupeptin, 5 mM DDT, 1 mM PMSF, 10  $\mu$ g/ml aprotinin and 10  $\mu$ g/ml pepstatin A] by freezing and thawing at –80  $^{\circ}$ C ( $\times$ 3). Lysates were then centrifuged (11,000 $\times$ g, 4  $^{\circ}$ C, 20 min) and the supernatants were boiled with 0.33 volumes of SDS/PAGE sample buffer. Protein concentrations were determined using the BioRad Bradford assay.

#### 2.4. Sub-cellular fractionation

Cytosolic and nuclear extracts were prepared as previously described [42] with slight modifications. Briefly, cells were harvested in Buffer A (10 mM HEPES, 10 mM KCl, 0.1 mM EGTA, 0.1 mM EDTA, 1.5 mM MgCl<sub>2</sub>, 10 mM NaF, 1 mM Na<sub>3</sub>VO<sub>4</sub>, 20 mM β-glycerophosphate, 2 μg/ml leupeptin, 1 mM DDT, 0.5 mM PMSF, 4 μg/ml aprotinin) and incubated on ice for 15 min. Samples were centrifuged (1400×g, 5 min, 4 °C) and the supernatants, containing the cytosolic fraction, were boiled with 0.33 volumes of SDS/PAGE sample buffer. Pellets were washed with Buffer A containing 0.6% (v/v) Nonidet P40 and centrifuged (1400×g, 5 min, 4 °C) to obtain pellets. Pellets were re-suspended in Buffer B (20 mM HEPES, 0.4 M NaCl, 1 mM EGTA, 0.1 mM EDTA, 1.5 mM MgCl<sub>2</sub>, 10 mM NaF, 1 mM Na<sub>3</sub>VO<sub>4</sub>, 20 mM β-glycerophosphate, 2 μg/ml leupeptin, 0.2 mM DDT, 0.5 mM PMSF, 4 μg/ml aprotinin) and incubated under rotation, for 1 h, at 4 °C. After centrifugation (11,000×g, 10 min, 4 °C), the supernatants containing the nuclear protein were either stored at –80 °C for use in electrophoretic mobility shift assays (EMSAs) or boiled with 0.33 volumes of SDS/PAGE sample buffer for use in Western blotting assays. Protein concentrations were determined using the BioRad Bradford assay.

#### 2.5. SDS-PAGE and immunoblot analysis

Proteins were separated by SDS-PAGE on 10% (w/v) acrylamide, 0.275% (w/v) bisacrylamide slab gels and transferred electrophoretically onto nitrocellulose membranes (0.45 μm). Membranes were then incubated in TBS-T [20 mM Tris–HCl, pH 7.5, 137 mM NaCl, 0.05% (v/v) Tween 20] containing 5% (w/v) non-fat milk powder for 30 min at room temperature. Subsequently, the membranes were incubated with the appropriate antibody according to the manufacturer's instructions. After washing in TBS-T (3 × 10 min), blots were incubated with horse-radish peroxidase-linked anti-rabbit or anti-mouse IgG antibodies [1:5000 dilution in TBS-T containing 1% (w/v) non-fat milk powder, 1 h, room temperature]. After washing again in TBS-T (3 × 10 min), bands were detected using enhance chemiluminescence and quantified by scanning densitometry (Gel Analyzer v.1.0).

#### 2.6. Electrophoretic mobility shift assays (EMSA)

The assay was performed as described by Markou et al. [43] with slight modifications. Briefly, oligonucleotides corresponding to the binding consensus sequences of NF-κB were annealed and 5' end-labelled with [γ-<sup>32</sup>P]ATP using T4 polynucleotide kinase. Unincorporated [γ-<sup>32</sup>P]ATP was removed using α Sephadex G50 column. Nuclear extracts (10 μg) were incubated (15 min, 4 °C) in binding buffer (5 mM MgCl<sub>2</sub>, 34 mM KCl and 0.15 μg/μl poly dI-dC). Subsequently, samples were incubated for 30 min at 4 °C with 100,000 cpm of labelled oligonucleotides. In supershift experiments, antibody against the NF-κB p65 subunit was added to nuclear extracts prior to binding (1 h, 4 °C). DNA-protein complexes were resolved in 4% polyacrylamide (29:1 acrylamide/bisacrylamide) gels, in 0.5× TBE buffer (890 mM Tris–HCl pH 8.0, 890 mM boric acid, 20 mM EDTA). Gels were dried and exposed to Super RX photo film at –80 °C for 24 h using an intensifying screen.

#### 2.7. MTT assay

Cell viability was estimated using the MTT assay [44]. Cells were seeded in 96-well culture plates and treated with the oxidant for 24 h. Four hours prior to the end of treatment, 50 μg MTT [3-(4,5-dimethylthiazol-2-yl)-2,5-diphenyltetrazolium bromide] were added to each well. Finally, cells were lysed in 0.1 M HCl in isopropanol and optical density was measured in an ELISA microplate reader (DENLEY, West Sussex, UK) using a 540 nm filter.

#### 2.8. DNA ladder detection

Detection of DNA ladder was performed according to the method described by Nguyen et al. [45] with minor modifications. Cells were centrifuged (600×g,

10 min) and washed with PBS. The cell pellet was re-suspended in suspension buffer (100 mM Tris–HCl, pH 8, 200 mM NaCl, 10 mM EDTA) and lysed by the addition of an equal volume of digestion buffer (100 mM Tris–HCl, pH 8, 200 mM NaCl, 10 mM EDTA, 0.4% SDS and 200 μg proteinase K). After an overnight incubation at 55 °C, DNA was extracted twice with a phenol–chloroform solution [1:1 (v/v)] and the aqueous phase was treated with RNase (20 μg/ml) for 30 min. DNA was precipitated with ice-cold ethanol and resolved in water. 5 μg DNA of each sample was subjected to electrophoresis on a 1% (w/v) agarose gel and visualised under ultraviolet light after 15 min incubation in ethidium bromide.

#### 2.9. Statistical evaluations

Western blots and EMSAs shown are representative of at least three independent experiments. All data are presented as means±S.E.M. Comparisons between control and treatments were performed using Student's unpaired *t*-test. A value of at least *P*<0.05 was considered to be statistically significant.

### 3. Results

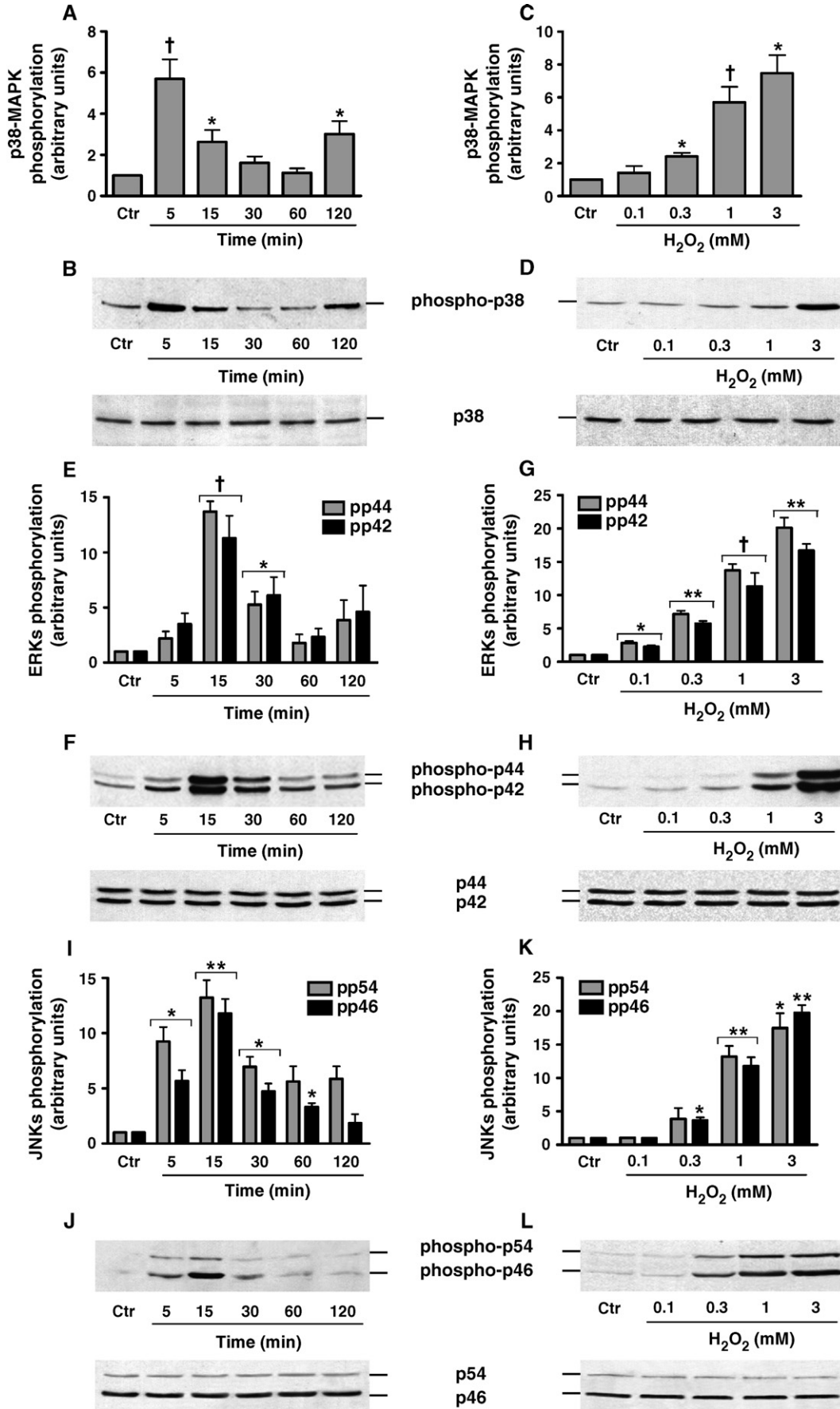
#### 3.1. ERKs, JNKs and p38-MAPKs subfamilies are activated by H<sub>2</sub>O<sub>2</sub> treatment

As the first step in the present study, the activation of MAPK subfamilies by H<sub>2</sub>O<sub>2</sub> using specific antibodies against the dually phosphorylated (hence, activated) forms of the kinases was examined. The results revealed that all three MAPK subfamilies examined are rapidly and strongly activated by H<sub>2</sub>O<sub>2</sub> treatment, following a time- and dose-dependent pattern. In particular, p38-MAPK activation displayed a rapid onset within 5 min of treatment (5.70±0.94 fold relative to controls, *P*<0.001), followed by a progressive decline, returning to basal levels within 30 min, while a second peak was observed (3.01±0.63-fold, relative to control values, *P*<0.05) at 120 min of treatment (Fig. 1A and B top panel). The minimal concentration of H<sub>2</sub>O<sub>2</sub> inducing a significant p38-MAPK activation was 0.3 mM (2.42±0.22-fold relative to controls, *P*<0.05). Increasing H<sub>2</sub>O<sub>2</sub> concentration led to increased p38-MAPK phosphorylation (7.47±1.1-fold relative to controls at 3 mM of H<sub>2</sub>O<sub>2</sub>, *P*<0.05) (Fig. 1C and D top panel).

Activation of ERKs by H<sub>2</sub>O<sub>2</sub> was intense, reaching maximum values within 15 min of treatment (13.71±0.94-fold relative to control values for p44 and 11.30±2.03-fold for p42, *P*<0.001), decreasing thereafter and reaching control levels at 60 min (Fig. 1E and F top panel). ERKs activation was induced by lower H<sub>2</sub>O<sub>2</sub> concentration (0.1 mM) than that of p38 (2.80±0.28-fold relative to control for p44 and 2.24±0.23-fold for p42, *P*<0.05) and maximal activation of the kinases was induced by 3 mM of the oxidant (20.12±1.51-fold for p44 and 16.70±1.01-fold for p42, *P*<0.01, respectively, above basal values) (Fig. 1G and H top panel).

Activation of JNKs was also observed at 5 min of H<sub>2</sub>O<sub>2</sub> treatment (9.26±1.3-fold, relative to control values for p54 and 5.66±0.99-fold for p46, *P*<0.05), reaching maximal levels at

Fig. 1. Effect of H<sub>2</sub>O<sub>2</sub> on MAPKs activation in skeletal myoblasts. C2 myoblasts were left untreated (Ctr) or were treated with 1 mM H<sub>2</sub>O<sub>2</sub> for the indicated times (A, B, E, F, I and J) or with various H<sub>2</sub>O<sub>2</sub> concentrations for 15 min (G, H, K and L) or for 5 min (C and D). The kinases were detected by immunoblotting, using specific antibodies against phospho-p38-MAPK (B and D top panels), p38-MAPK (B and D bottom panels), phospho-ERK1/2 (F and H top panels), ERK1/2 (F and H bottom panels), phospho-JNK1/2 (J and L top panels) and JNK1/2 (J and L bottom panels). Phospho-MAPK bands were quantified by laser scanning densitometry and the results are presented as fold-relative to control values (A, C, E, G, I and K). \**P*<0.05, \*\**P*<0.01, †*P*<0.001 vs. control value.



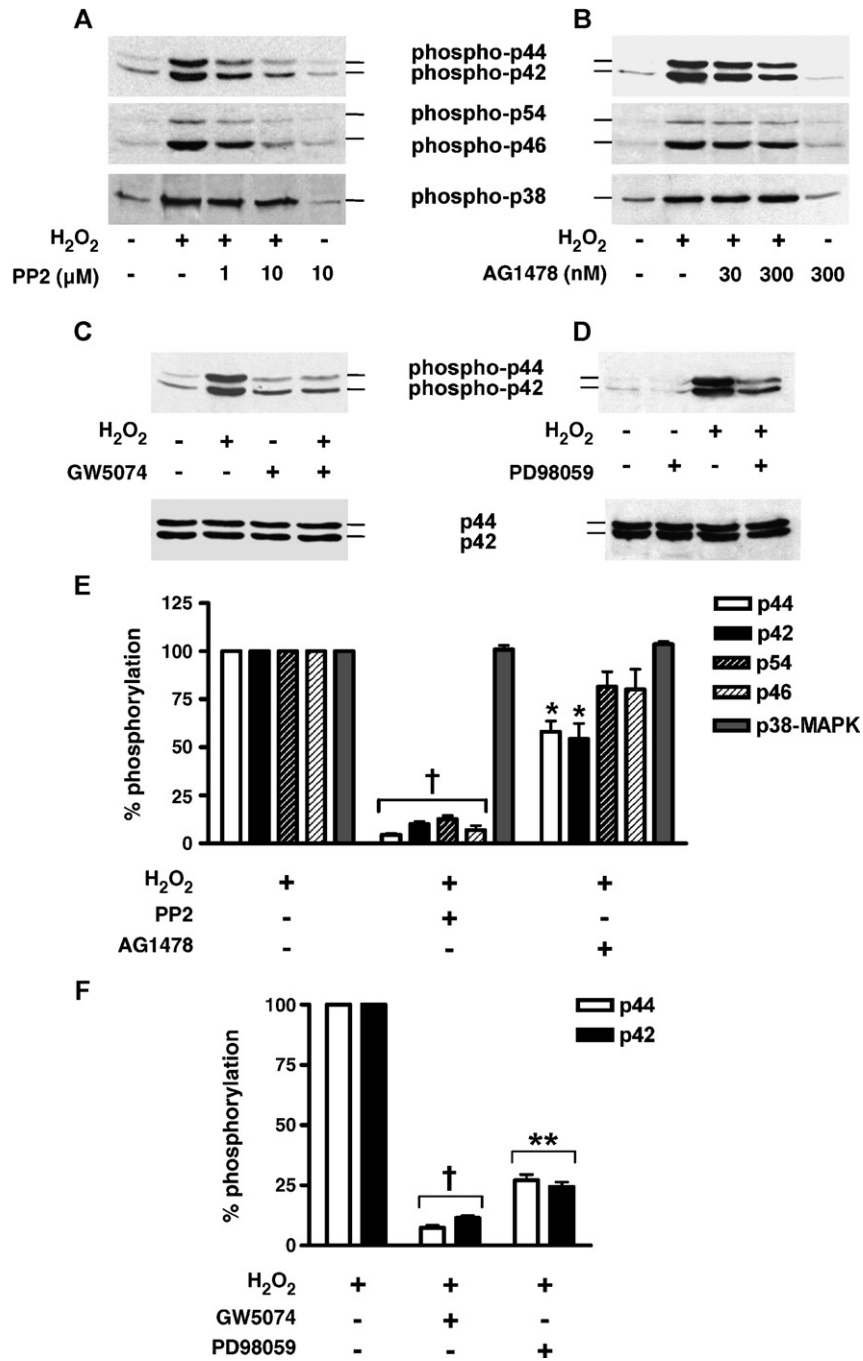


Fig. 2. Effect of pharmacological inhibitors on MAPKs pathways. Cells were treated with 1 mM of H<sub>2</sub>O<sub>2</sub> for 15 min (A and B top and middle panels; C and D) or for 5 min (A and B bottom panels), in the absence or presence of the following inhibitors: PP2 (1 and 10 μM), AG1478 (30 and 300 nM), GW5074 (2.5 μM) or PD98059 (25 μM). The kinases were detected by immunoblotting, using specific antibodies against phospho-ERKs (A, B, C and D top panels), phospho-JNKs (A and B middle panels), phospho-p38-MAPK (A and B bottom panels) and ERKs (C and D bottom panels). Phospho-MAPK bands were quantified by laser scanning densitometry and the results are presented as percentage of phosphorylation compared to the phosphorylation induced by H<sub>2</sub>O<sub>2</sub> (positive control), which is set to 100 (E and F). \**P*<0.05, \*\**P*<0.01, †*P*<0.001 vs. positive control value.

15 min (13.22±1.57-fold relative to controls for p54 and 11.78±1.31-fold for p46, *P*<0.01) with a progressive decrease thereafter (Fig. 1I and J top panel). JNKs activation followed a H<sub>2</sub>O<sub>2</sub> dose-dependent activation pattern (Fig. 1K and L top panel). Statistically significant activation was observed at 0.3 mM H<sub>2</sub>O<sub>2</sub> for p46 (3.67±0.43-fold relative to controls, *P*<0.05) and at 1 mM H<sub>2</sub>O<sub>2</sub> for p54 (13.22±1.57-fold relative to control, *P*<0.01). Their activation during treatment with 3 mM H<sub>2</sub>O<sub>2</sub> was 17.49±

2.19-fold relative to controls (*P*<0.05) for p54 and 19.76±1.15-fold (*P*<0.01) for p46.

The above results indicate that H<sub>2</sub>O<sub>2</sub> induces a differential activation of the three well-established MAPK subfamilies, in relation to both time of exposure and dose of the oxidant. Bottom panels in Fig. 1 show that there were no changes in the total cellular pools of all MAPKs examined and, therefore, provide a control for equal protein loading under these conditions.

3.2. Src and, partially, EGFR mediate the phosphorylation of ERKs and JNKs, but not that of p38-MAPK

Although MAPK activation during oxidative stress has been studied in detail in diverse cell types, the signalling pathways

leading to their phosphorylation under such conditions are not yet clarified. To date, there is no evidence about the mechanisms of oxidative stress-induced MAPK activation in skeletal muscle cells. In order to study these pathways, pharmacological inhibitors of various kinases were used, based on literature data. The results

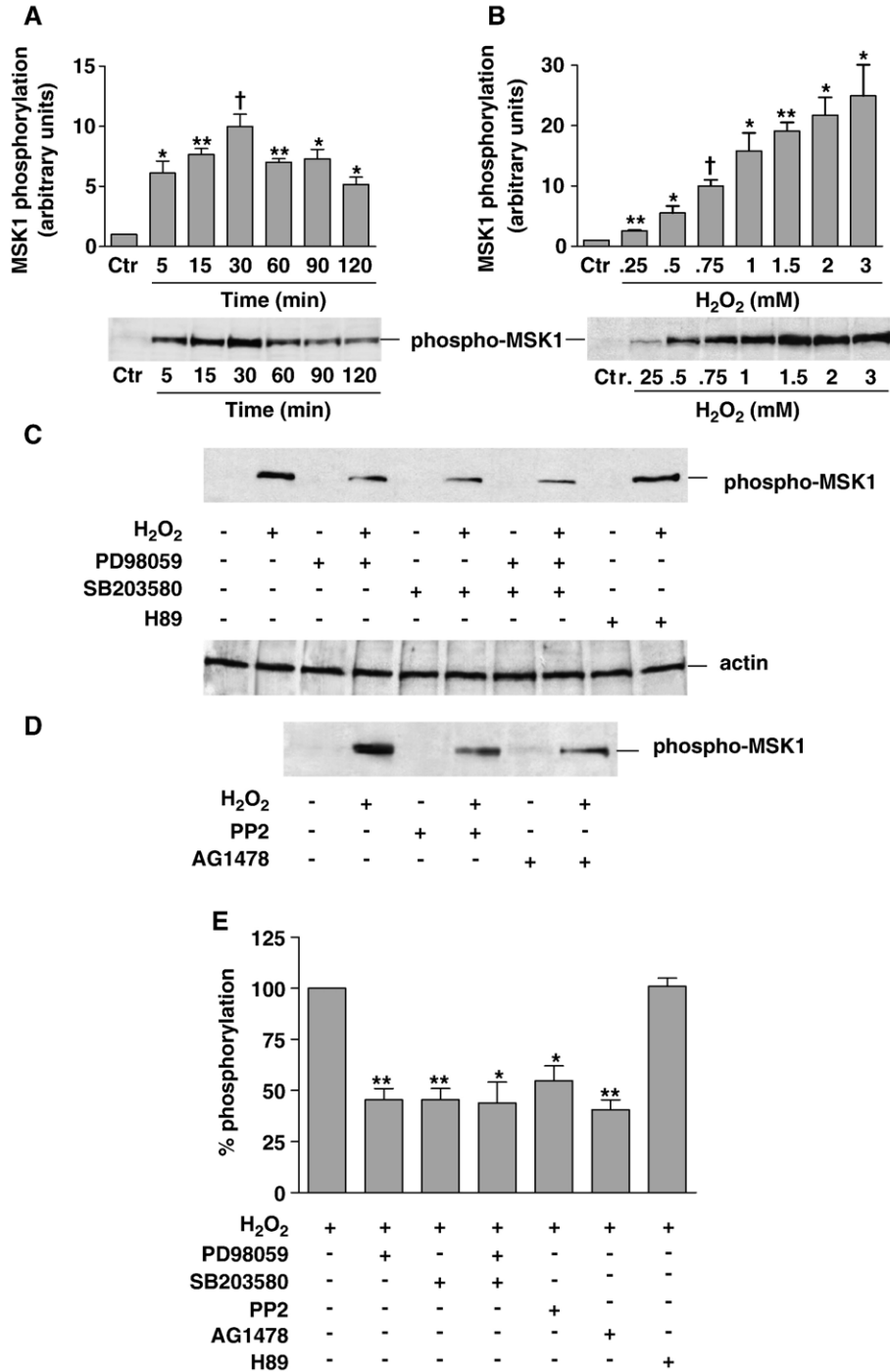


Fig. 3. MSK1 activation by H<sub>2</sub>O<sub>2</sub>. Cells were left untreated (Ctr) or treated with 0.75 mM of H<sub>2</sub>O<sub>2</sub> for various time periods (A) or with various concentrations of H<sub>2</sub>O<sub>2</sub> for 30 min (B). Phosphorylation of MSK1 was examined by immunoblotting, using a specific antibody against the phosphorylated form of the kinase. Densitometric analysis of phosphorylation as well as the respective representative immunoblots are shown. (C, D) Cells were treated for 30 min with 0.75 mM of H<sub>2</sub>O<sub>2</sub> in the absence or presence of the following inhibitors: PD98059 (25 μM), SB203580 (10 μM), H89 (10 μM), PP2 (10 μM) or AG1478 (300 nM). Immunoblotting was performed using an antibody against phospho-MSK1. (E) Densitometric analysis of MSK1 phosphorylation in the presence of various inhibitors is presented as percentage of phosphorylation compared to the phosphorylation induced by H<sub>2</sub>O<sub>2</sub> (positive control), which is set to 100. Actin is used as a loading control (C bottom panel). \**P*<0.05, \*\**P*<0.01, †*P*<0.001 vs. control (A and B) or vs. positive control (E) value.

of these experiments showed that 10  $\mu$ M PP2 (a specific inhibitor of Src kinases) abolishes the activation of ERKs (Fig. 2A top panel and E) and JNKs (Fig. 2A middle panel and E) induced by 1 mM  $H_2O_2$ , whereas this inhibitor had no effect on p38-MAPK activation (Fig. 2A bottom panel and E). Moreover, 300 nM AG1478 (a specific EGFR inhibitor) resulted in a partial inhibition of ERKs (41.99% reduction for p44 and 45.76% for p42,  $P < 0.05$ ) (Fig. 2B top panel and E), whereas it had not any significant inhibitory effect on JNKs activation by  $H_2O_2$  (Fig. 2B middle panel and E). Once more, p38-MAPK phosphorylation was not affected by this inhibitor (Fig. 2B bottom panel and E). To investigate whether the signalling pathway leading to ERK and JNK activation was Ras-Raf-mediated, GW5074 (a specific inhibitor of cRaf1) was used. 2.5  $\mu$ M of GW5074 diminished the activation of ERKs induced by  $H_2O_2$  (Fig. 2C top panel and F), while it had no effect on the activation of JNKs induced by 1 mM  $H_2O_2$  (data not shown). Finally, 25  $\mu$ M of PD98059 (a selective MEK1/2 inhibitor) significantly reduced, as it was expected, the activation of ERKs by  $H_2O_2$  (Fig. 2D top panel and F). The above results demonstrate that the activation mechanisms of ERKs and JNKs by  $H_2O_2$  comprise common components, such as the Src kinase. On the contrary, the activation pathway of p38-MAPK by  $H_2O_2$  seems to be Src kinase-independent.

### 3.3. ERKs and p38-MAPK mediate the phosphorylation of MSK1 by $H_2O_2$

MSK1 is a substrate of ERKs and p38-MAPK and it was found to phosphorylate the p65 subunit of NF- $\kappa$ B at Ser276 during TNF- $\alpha$  stimulation [35]. Therefore, phosphorylation of MSK1 (at Thr581) was investigated during  $H_2O_2$  treatment of C2 myoblasts. As shown in Fig. 3A, the kinase was phosphorylated rapidly, within 5 min ( $6.11 \pm 0.99$ -fold relative to control values,  $P < 0.05$ ), reaching maximal phosphorylation levels after 30 min of treatment ( $9.98 \pm 1.03$ -fold relative to controls,  $P < 0.001$ ). This

phosphorylation declined thereafter, but remained considerably above basal levels for at least 2 h of treatment. A concentration of 0.25 mM of  $H_2O_2$  was sufficient to induce MSK1 phosphorylation ( $2.56 \pm 0.14$ -fold relative to control values,  $P < 0.01$ ), which was maximized at 3 mM of  $H_2O_2$  ( $24.94 \pm 5.14$ -fold relative to controls,  $P < 0.05$ ) (Fig. 3B). It appears, therefore, that the phosphorylation pattern of MSK1 resembles that of MAPKs.

The inhibitor of MEK1/2, and consequently of ERKs, PD98059 and the inhibitor of p38-MAPK, SB203580, resulted in a significant decrease in  $H_2O_2$ -mediated phosphorylation of MSK1 ( $54.52 \pm 5.38\%$  reduction with PD98059 and  $54.5 \pm 5.49\%$  reduction with SB203580,  $P < 0.01$ ) (Fig. 3C top panel and E). Interestingly, simultaneous use of both inhibitors of ERKs and p38-MAPK did not result in a significant additive effect (Fig. 3C top panel and E). Furthermore, we examined the effect of the inhibitors of ERK1/2 upstream activators, Src and EGFR, on MSK1 phosphorylation. A considerable decrease in  $H_2O_2$ -induced phosphorylation of MSK1 by 10  $\mu$ M PP2 ( $45.23 \pm 7.25\%$  reduction,  $P < 0.05$ ) or 300 nM AG1478 ( $59.44 \pm 4.83\%$  reduction,  $P < 0.01$ ) was observed (Fig. 3D and E). It has been shown that the inhibitor of MSK1, H89, affects only the activity of the kinase but not its phosphorylation levels [46]. In accordance with this finding, H89 had no effect on the  $H_2O_2$ -induced MSK1 phosphorylation (Fig. 3C top panel and E). The results of these experiments indicate that MSK1 is strongly phosphorylated by ERKs and p38-MAPK during  $H_2O_2$  treatment and may play a role in myoblast response to oxidative stress.

### 3.4. NF- $\kappa$ B is activated by $H_2O_2$ in skeletal myoblasts

We next studied the activation pattern of NF- $\kappa$ B by  $H_2O_2$ . To this end, cells were treated with increasing concentrations of  $H_2O_2$  for 2 h, or with 1 mM  $H_2O_2$  for various time periods. Nuclear extracts were prepared and subjected to EMSA, to test the DNA binding activity of the nuclear factor. 0.25 mM  $H_2O_2$  induced a moderate activation of NF- $\kappa$ B, which increased in a dose-

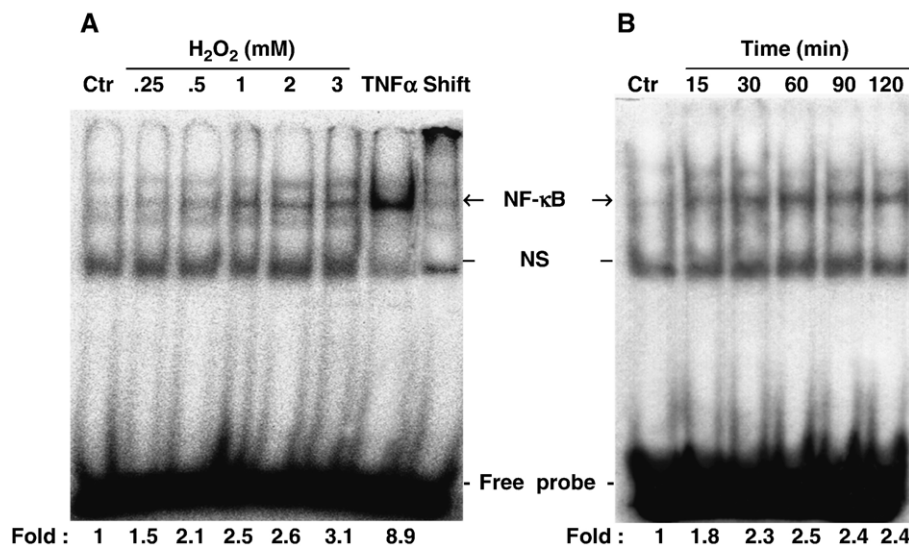


Fig. 4. Effect of  $H_2O_2$  on NF- $\kappa$ B binding activity in skeletal myoblasts. (A) Nuclear extracts were prepared from myoblasts treated with increasing concentrations of  $H_2O_2$  for 1 h and subjected to EMSA. Extracts from cells treated for 30 min with 1000 U/ml TNF- $\alpha$  were used as positive controls (lane: TNF- $\alpha$ ). Pre-incubation of nuclear extracts, following the TNF- $\alpha$  treatment, with an anti-p65 antibody, resulted to a super-shifted band of NF- $\kappa$ B (last lane). (B) EMSA of nuclear extracts of myoblasts after treatment with 1 mM  $H_2O_2$  for increasing time periods (Ctr: control, NS: non specific binding).

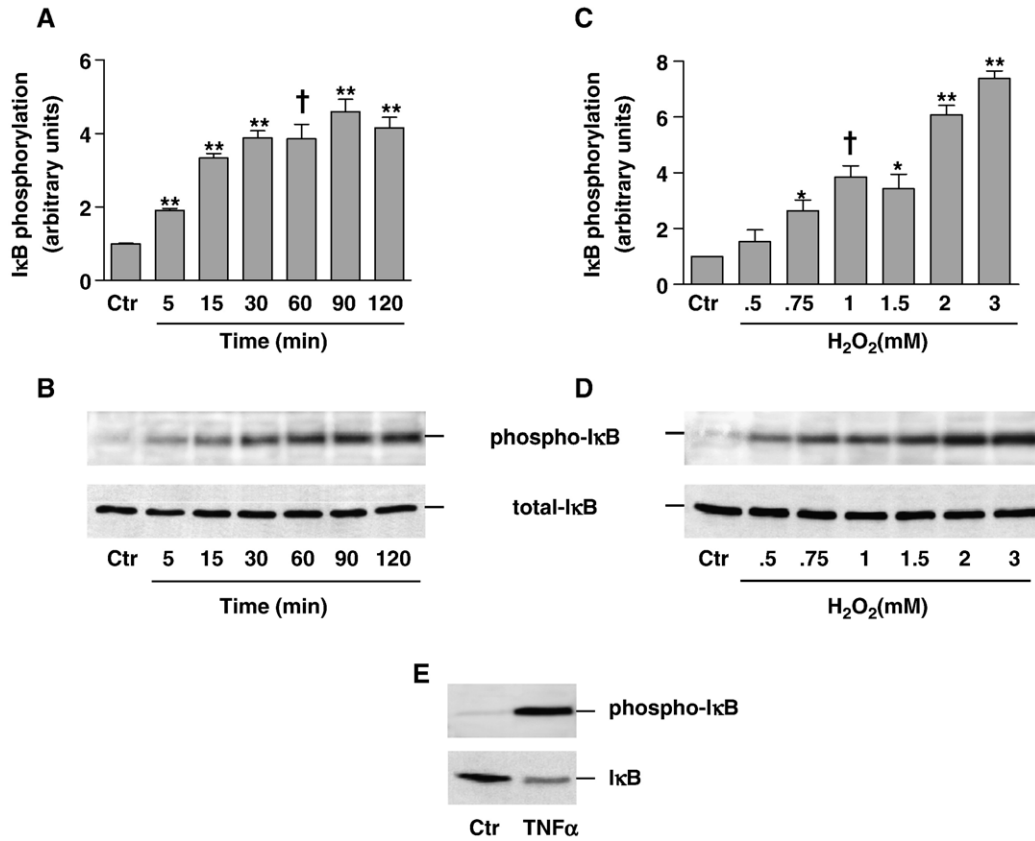


Fig. 5. Effect of H<sub>2</sub>O<sub>2</sub> on IκB phosphorylation and degradation. Cells were treated with 1 mM H<sub>2</sub>O<sub>2</sub> for various time intervals (B) or with increasing concentrations of H<sub>2</sub>O<sub>2</sub> for 1 h (D) or with 1000 U/ml TNF-α for 30 min (E). IκB phosphorylation was assessed by immunoblotting using a specific anti-phospho (Ser32/36)-IκB-α antibody (B, D and E top panels) and total IκB levels were measured using an antibody against total IκB-α (B, D and E bottom panels). Densitometric analysis of the phosphorylated IκB bands during H<sub>2</sub>O<sub>2</sub> treatments is also presented (A and C). \**P*<0.05, \*\**P*<0.01, †*P*<0.001 vs. control value.

dependent manner (Fig. 4A). H<sub>2</sub>O<sub>2</sub>-induced NF-κB activation was also time-dependent, displaying an onset within 15 min, reaching maximal values within 1 h and remaining considerably above basal levels for at least 2 h of treatment (Fig. 4B). Nuclear extracts prepared from cells treated with TNF-α (1000 U/ml) for

30 min were used as positive controls (Fig. 4A). To confirm binding specificity, we used an antibody against the p65 subunit of NF-κB. Pre-incubation of nuclear extracts with the antibody led to a shift of the band to high molecular mass (Fig. 4A). These results reveal that NF-κB is activated by H<sub>2</sub>O<sub>2</sub> and translocates

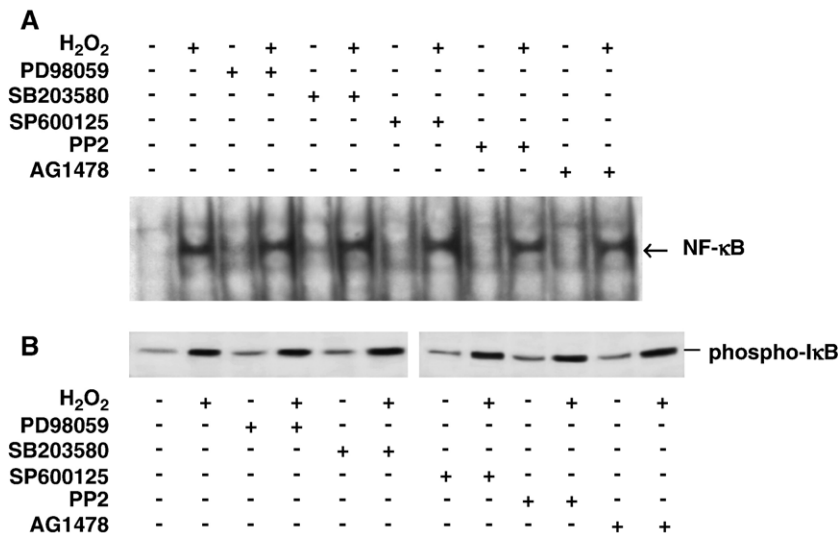


Fig. 6. Effect of MAPK inhibition on NF-κB DNA binding activity and IκB phosphorylation. Cells were treated with 1 mM H<sub>2</sub>O<sub>2</sub> for 1 h in the absence or presence of the following inhibitors: PD98059 (25 μM), SB203580 (10 μM), SP600125 (10 μM), PP2 (10 μM) or AG1478 (300 nM). (A) Nuclear extracts were prepared and subjected to EMSA. (B) Immunoblotting was performed using an antibody against the phosphorylated form of IκB.

into the nucleus. This activation, however, is weaker compared to the one observed during treatment with its potent inducer, TNF- $\alpha$ .

### 3.5. $H_2O_2$ induces phosphorylation, but not degradation, of I $\kappa$ B- $\alpha$

Phosphorylation and subsequent degradation of I $\kappa$ B is required for NF- $\kappa$ B activation, according to the classical activation pathway. Therefore, I $\kappa$ B phosphorylation was examined, using a specific antibody against the phosphorylated (Ser 32/36) form of I $\kappa$ B- $\alpha$ . We found that I $\kappa$ B was phosphorylated during  $H_2O_2$  treatment, in a time- and dose-dependent profile. This phosphorylation was rapid, within 5 min of treatment ( $1.91 \pm 0.05$ -fold relative to controls,  $P < 0.01$ ), reached maximal values within 30 min ( $3.88 \pm 0.19$ -fold relative to controls,  $P < 0.01$ ) and remained at maximum levels for at least 2 h (Fig. 5A and B top panel). Phosphorylation of I $\kappa$ B could be detected when concentration of  $H_2O_2$  used was 0.5 mM or higher. Increasing  $H_2O_2$  concentration induced increasing I $\kappa$ B phosphorylation (reaching  $7.39 \pm 0.27$ -fold relative to controls,  $P < 0.01$ , at 3 mM  $H_2O_2$ ) (Fig. 5C and D top panel). Thus, we

observed that the phosphorylation pattern of I $\kappa$ B complies with  $H_2O_2$ -induced DNA binding activity of NF- $\kappa$ B.

However, when total I $\kappa$ B levels were examined, using a specific antibody, there was not any apparent decrease at all time points (Fig. 5B bottom panel) and  $H_2O_2$  concentrations (Fig. 5D bottom panel) tested. This result suggests that there is not any significant degradation of I $\kappa$ B during  $H_2O_2$  treatment. As a positive control for I $\kappa$ B degradation, cells treated with TNF- $\alpha$  were used. A slightly stronger phosphorylation of I $\kappa$ B was detected, compared to that induced by  $H_2O_2$ , as well as a considerable decrease in I $\kappa$ B total levels (Fig. 5E). It seems, therefore, that there are differences in the activation mechanism of NF- $\kappa$ B by  $H_2O_2$  compared to that induced by TNF- $\alpha$ .

### 3.6. MAPKs are not implicated in nuclear translocation of NF- $\kappa$ B

To investigate the possible cross talk between NF- $\kappa$ B and MAPKs pathways, we initially examined the effect of MAPK selective inhibitors on DNA binding activity of NF- $\kappa$ B during

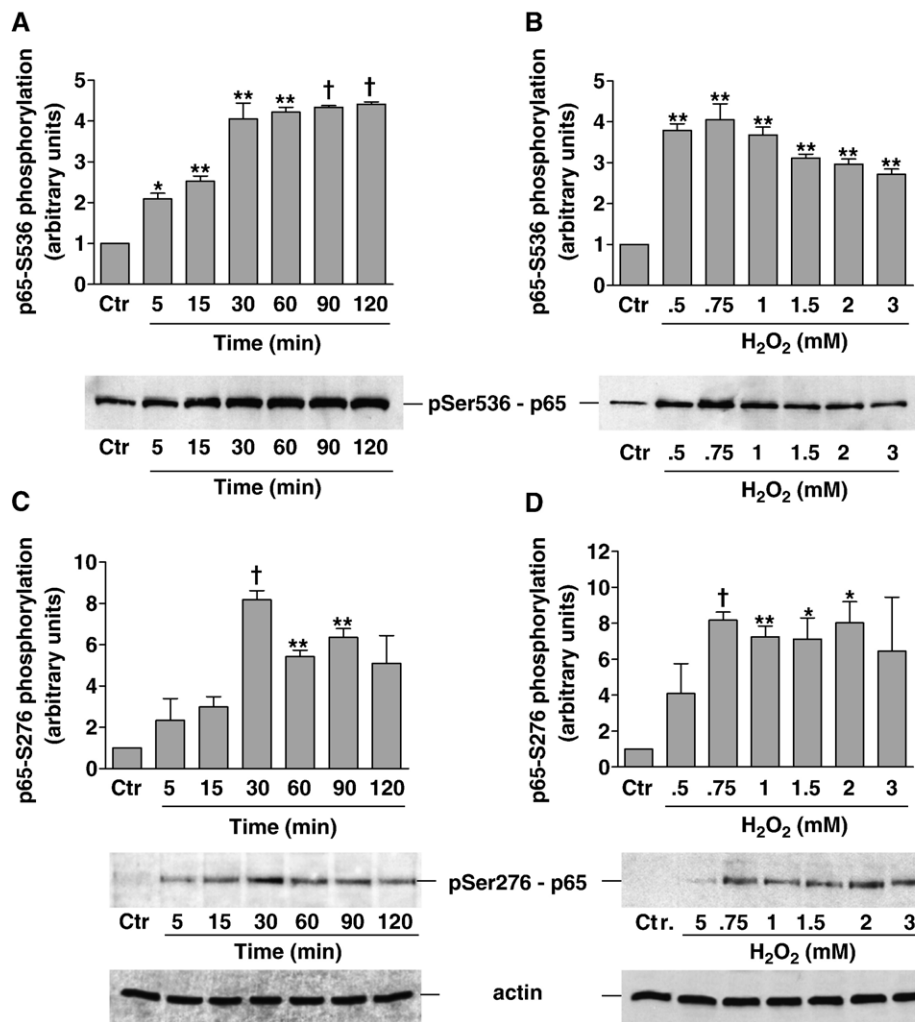


Fig. 7.  $H_2O_2$  mediates the phosphorylation of p65. Cells were left untreated (Ctr) or treated with 0.75 mM of  $H_2O_2$  for various time periods (A and C top panel) or with various oxidant concentrations for 30 min (B and D top panel). Phosphorylation of p65 was examined by immunoblotting, using two specific antibodies against phospho-Ser536-p65 (A and B) and phospho-Ser276-p65 (C and D). Densitometric analysis of phosphorylation as well as the respective representative immunoblots are shown. Actin is used as a loading control (C and D bottom panels). \* $P < 0.05$ , \*\* $P < 0.01$ , † $P < 0.001$  vs. control value.

H<sub>2</sub>O<sub>2</sub> treatment. There was not any significant alteration of the H<sub>2</sub>O<sub>2</sub>-induced activation of NF- $\kappa$ B when the cells were pretreated with the inhibitors of ERKs, JNKs, p38-MAPK, Src and EGFR (Fig. 6A). Moreover, none of the above inhibitors affected I $\kappa$ B phosphorylation (Fig. 6B). These results suggest that MAPKs pathways are not involved in the nuclear translocation of the transcription factor during H<sub>2</sub>O<sub>2</sub> stimulation.

### 3.7. NF- $\kappa$ B p65 subunit is phosphorylated at Ser536 and Ser276 during stimulation with H<sub>2</sub>O<sub>2</sub>

Activation of NF- $\kappa$ B involves not only dissociation from I $\kappa$ B but also transactivation through post-translational modifications of its p65 subunit. Thus, to further investigate the activation of NF- $\kappa$ B and the possible interactions with MAPKs, the phosphorylation status of two main p65 phosphorylation sites, Ser276 and Ser536, was examined. These residues were chosen since there are reports suggesting that they are substrates of MSK1 and RSK1, respectively, kinases downstream of MAPK pathways [35,36]. We found that H<sub>2</sub>O<sub>2</sub> induced a time- and dose-dependent phosphorylation of both residues, but with quite different profiles. Phosphorylation at Ser536 was rapid, within 5 min of treatment ( $2.09 \pm 0.14$ -fold relative to controls,  $P < 0.05$ ). Maximal phosphorylation of this residue was observed 30 min ( $4.05 \pm 0.39$ -fold relative to control values,  $P < 0.01$ ) after the onset of the treatment, remaining at these maximum levels for at least 2 h (Fig. 7A). The concentration of H<sub>2</sub>O<sub>2</sub> inducing maximal Ser536 phosphorylation was 0.75 mM ( $4.05 \pm 0.39$ -fold relative to controls,  $P < 0.01$ ), while further increase of its concentration resulted in a progressive decrease of this phosphorylation, remaining, though, above basal levels (Fig. 7B).

Significant phosphorylation of p65 at Ser276 was induced at a later time point (30 min), but was stronger ( $8.18 \pm 0.45$ -fold relative to controls,  $P < 0.001$ ), compared to the phosphorylation at Ser536. A decrease of Ser276 phosphorylation was observed thereafter, although it remained above control levels, even after 2 h of treatment (Fig. 7C). Phosphorylation of Ser276 during treatment with increasing H<sub>2</sub>O<sub>2</sub> concentrations displayed a maximum at 0.75 mM and remained at maximal levels during further increase of H<sub>2</sub>O<sub>2</sub> concentration (Fig. 7D). These results demonstrate that p65 subunit of NF- $\kappa$ B is phosphorylated at least at two different serine residues during H<sub>2</sub>O<sub>2</sub> treatment. The phosphorylation pattern of these residues is different and, it seems that, the one of Ser276, but not that of Ser536, is comparable with the activation profile of MAPKs.

### 3.8. p65 phosphorylation at Ser536 is Src-dependent

To investigate whether there are interactions between NF- $\kappa$ B and MAPKs pathways at the transactivation level, we used inhibitors of MAPKs cascades and examined their effect on H<sub>2</sub>O<sub>2</sub>-induced p65 phosphorylations. Concerning Ser536 phosphorylation, we observed that inhibition of ERKs, JNKs and p38-MAPK, using their selective inhibitors PD98059, SP600125 and SB203580, respectively, had no effect on H<sub>2</sub>O<sub>2</sub>-induced phosphorylation of this residue (Fig. 8A top panel and C). On the contrary, Src inhibitor, PP2, considerably reduced H<sub>2</sub>O<sub>2</sub>-induced phosphorylation of Ser536 ( $44.99 \pm 1.62\%$  reduction,  $P < 0.01$ ), whereas EGFR inhibitor, AG1478, did not cause any significant

decrease of Ser536 phosphorylation (Fig. 8B and C). These results imply that this residue is not a direct or indirect substrate of any MAPK subfamily, although there are common upstream activators (such as Src) of p65 (Ser536), ERKs and JNKs.

### 3.9. Phosphorylation of p65 at Ser276 is MSK1-mediated

We further examined the effect of MAPK pathways inhibitors on H<sub>2</sub>O<sub>2</sub>-induced phosphorylation of p65 at the second amino acid residue (Ser276). While JNK inhibitor SP600125 did not affect this phosphorylation (data not shown), inhibition of ERKs and p38-MAPK, by PD98059 and SB203580, respectively, resulted in a significant reduction of Ser276 phosphorylation ( $67.5 \pm 4.25\%$  reduction by PD98059 and  $63.4 \pm 6.05\%$  reduction by SB203580,  $P < 0.01$ ) (Fig. 9A top panel and C). The use of both inhibitors simultaneously, however, did not exhibit any additive effect (Fig. 9A top panel and C). Furthermore, the effect of Src and EGFR inhibitors, PP2 and AG1478, respectively, on Ser276 phosphorylation was examined. In both cases, the H<sub>2</sub>O<sub>2</sub>-induced phosphorylation of this residue was decreased ( $68.42 \pm 4.19\%$  reduction by PP2,  $P < 0.01$ , and  $44.15 \pm 9.42\%$  reduction by AG1478,  $P < 0.05$ ) (Fig. 9B and C). Finally, the effect of the potent MSK1 inhibitor H89 was studied. This inhibitor diminished the phosphorylation of Ser276 by H<sub>2</sub>O<sub>2</sub> ( $82.67 \pm 3.1\%$  reduction,  $P < 0.01$ )

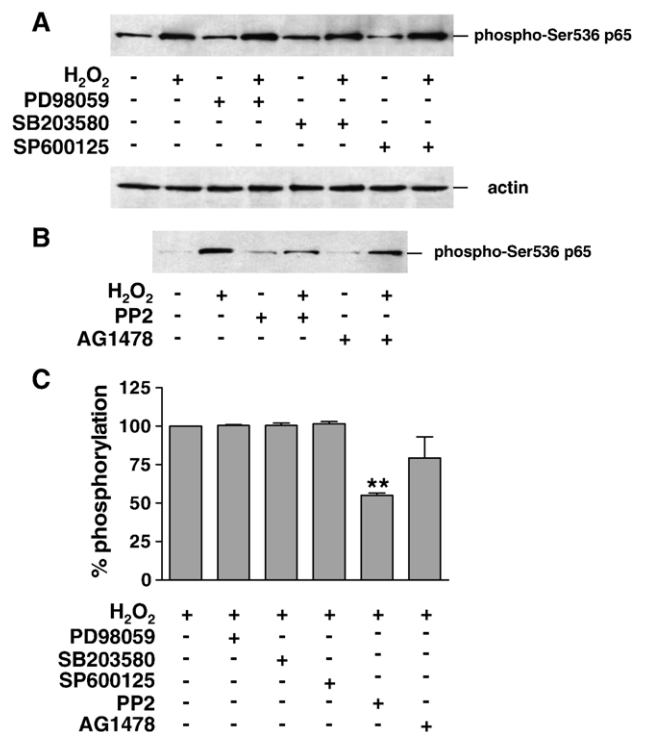


Fig. 8. Effect of MAPKs inhibitors on Ser536-p65 phosphorylation. Cells were treated with 0.75 mM of H<sub>2</sub>O<sub>2</sub> for 30 min in the absence or presence of the following inhibitors: PD98059 (25  $\mu$ M), SB203580 (10  $\mu$ M), SP600125 (10  $\mu$ M), PP2 (10  $\mu$ M) or AG1478 (300 nM). The phosphorylation of Ser536-p65 was detected by immunoblotting, using a specific antibody (A top panel and B). Actin is used as a loading control (A bottom panel). (C) Densitometric analysis of Ser536 phosphorylation in the presence of various inhibitors is presented, as percentage of phosphorylation compared to the phosphorylation induced by H<sub>2</sub>O<sub>2</sub> (positive control), which is set to 100. \*\* $P < 0.01$  vs. positive control value.

(Fig. 9A top panel and C). As it is suggested by these results, ERK and p38-MAPK are implicated in H<sub>2</sub>O<sub>2</sub>-induced phosphorylation of p65 at Ser276 and probably this phosphorylation is MSK1-mediated. Consequently, although there is not any interaction between NF- $\kappa$ B and MAPKs at the level of NF- $\kappa$ B translocation to the nucleus, it seems that there is a cross talk between these pathways at the NF- $\kappa$ B transactivation level.

### 3.10. H<sub>2</sub>O<sub>2</sub>-induced cell death of myoblasts is probably not related to apoptotic events

To estimate the effect of H<sub>2</sub>O<sub>2</sub> on myoblast viability, cells were treated with the oxidant for 24 h and subjected to MTT assay. Cell viability was not affected by H<sub>2</sub>O<sub>2</sub> treatment, except when high doses (at least 1 mM) were used (Fig. 10A). To investigate whether apoptotic mechanisms are implicated, we examined the activation of caspase-3 using an antibody against its active peptide and additionally, we performed the DNA fragmentation assay. Caspase-3 was not activated by H<sub>2</sub>O<sub>2</sub> (Fig. 10B) and DNA did not display the characteristic apoptotic laddering pattern (Fig. 10C). The above results, taken together, suggest that high H<sub>2</sub>O<sub>2</sub> con-

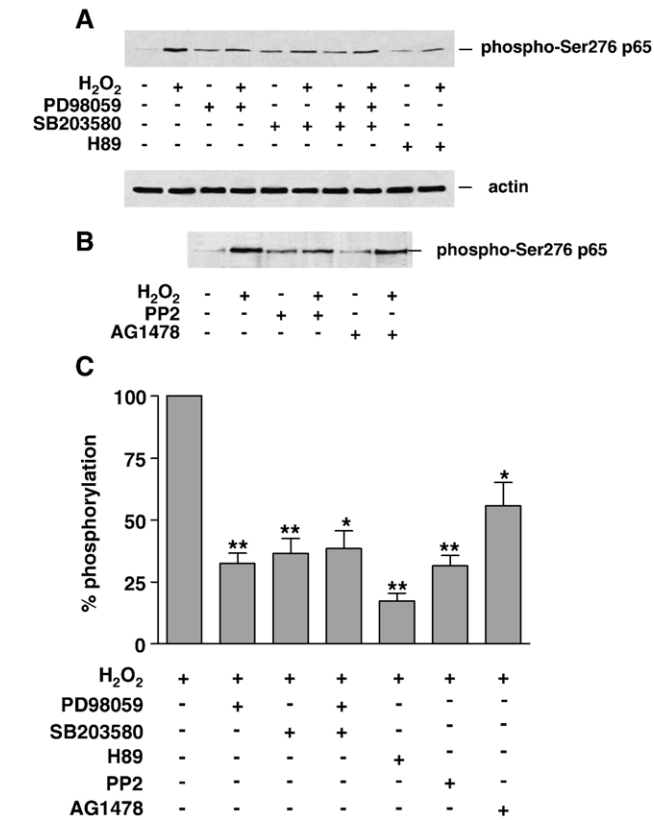


Fig. 9. Effect of MAPKs inhibitors on Ser276-p65 phosphorylation. Cells were treated with 0.75 mM of H<sub>2</sub>O<sub>2</sub> for 30 min in the absence or presence of the following inhibitors: PD98059 (25  $\mu$ M), SB203580 (10  $\mu$ M), H89 (10  $\mu$ M), PP2 (10  $\mu$ M) or AG1478 (300 nM). The phosphorylation of Ser276-p65 was detected by immunoblotting, using a specific antibody (A top panel and B). Actin is used as a loading control (A bottom panel). (C) Densitometric analysis of Ser276 phosphorylation in the presence of various inhibitors is presented, as percentage of phosphorylation compared to the phosphorylation induced by H<sub>2</sub>O<sub>2</sub> (positive control), which is set to 100. \* $P$ <0.05, \*\* $P$ <0.01 vs. positive control value.

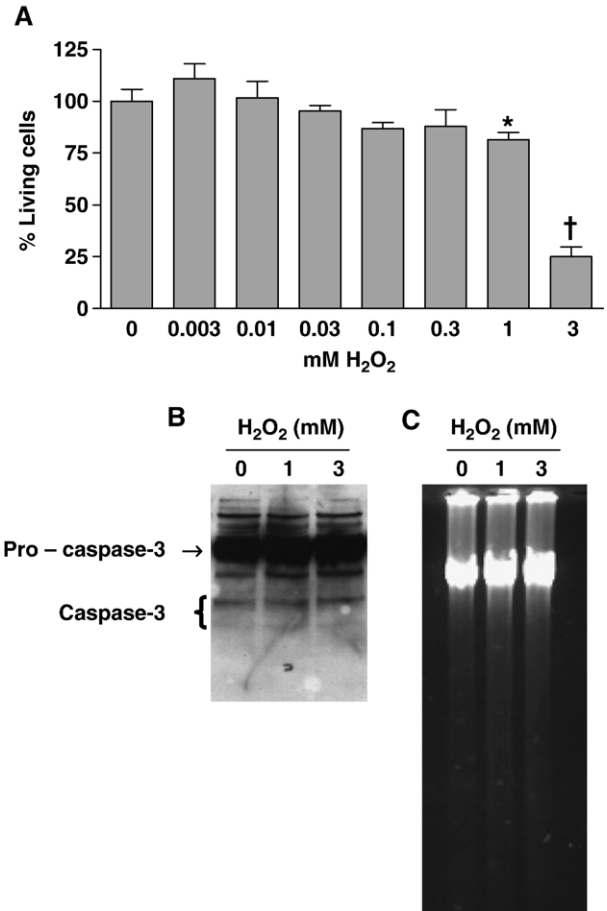


Fig. 10. Effect of H<sub>2</sub>O<sub>2</sub> on C2 myoblast viability. Cells were treated with various concentrations of H<sub>2</sub>O<sub>2</sub> for 24 h. (A) A MTT assay was performed and the results are presented as percentage over controls (untreated cells). (B) Activated caspase-3 was detected using an antibody against its active fragment. (C) DNA was extracted and electrophoresed on a 1% agarose gel for the detection of DNA ladder. \* $P$ <0.05, † $P$ <0.001 vs. control value.

centrations (i.e. 3 mM) induce necrosis of skeletal myoblasts rather than apoptosis.

## 4. Discussion

Skeletal muscle cells are capable of adapting to intense redox imbalances [3] and, therefore, they represent an ideal experimental system in studying the mechanisms during oxidative stress. As it has been shown in various studies, exogenously added oxidative compounds display a moderate effect on these cells' viability, even at quite high concentrations [47,48], a result revealing their "tolerance" during acute accumulation of ROS. However, the mechanisms implicated in this response are not well defined and, thus, the investigation of the pathways regulating the cellular function during oxidative stress is very important. For this purpose, we studied the effect of H<sub>2</sub>O<sub>2</sub> on two major pathways, MAPK and NF- $\kappa$ B, respectively, in C2 skeletal myoblasts.

We observed that treatment of C2 myoblasts with H<sub>2</sub>O<sub>2</sub> strongly activated the three well-established MAPK subfamilies examined, in a dose- and time-dependent manner (Fig. 1). Increasing concentrations of H<sub>2</sub>O<sub>2</sub> resulted in increased MAPK

activation. However, the time-course of this activation differed among the MAPK subfamilies. Activation of ERKs and JNKs was transient, maximized at 15 min, declining thereafter. On the other hand, p38-MAPK activation was more rapid, maximizing within 5 min and displaying a biphasic pattern, with a second peak obtained at 2 h of treatment. This p38-MAPK re-activation could be attributed to a feedback mechanism, mediated by its either upstream activators or downstream targets, a phenomenon that has been previously reported (p38 is also known as reactivating kinase—RK) [14,49,50].

A question remaining unanswered is whether different cell types share similar activation mechanisms of MAPKs pathways. EGFR and Src kinases have been shown to mediate ROS-induced MAPK activation in vascular endothelial cells [20], renal epithelial cells [21], cardiomyocytes and heart fibroblasts [22]. Our results point as well to a Src-dependent activation of ERKs and JNKs by H<sub>2</sub>O<sub>2</sub> in skeletal myoblasts (Fig. 2). Whether, in our experimental system, Src and EGFR lie in the same pathway leading to MAPK activation is under investigation. In agreement with Purdom and Chen [22], we observed that PP2 (a Src kinase inhibitor) displayed much higher efficiency inhibiting MAPK activation than AG1478 (an EGFR inhibitor) (Fig. 2). Src kinase is a well-known downstream target of EGFR tyrosine kinase [51]. Conversely, it has been shown that Src kinase can phosphorylate EGFR at Tyr845, stabilizing the activated state of the kinase domain, leading, consequently, to the activation of the MAPK cascade [20,52]. Therefore, in the case of a ligand-independent activation of EGFR, the sequential relationship between Src kinase and EGFR is not yet clarified.

H<sub>2</sub>O<sub>2</sub>-induced p38-MAPK phosphorylation was not affected by the above inhibitors, implying the existence of a completely different activation mechanism for this kinase. It is possible that

activation of p38-MAPK is regulated by Trx and ASK1 proteins [23], although this hypothesis remains to be elucidated.

Our results also indicate that MSK1 is strongly phosphorylated by H<sub>2</sub>O<sub>2</sub> treatment and that this phosphorylation is mediated by both, ERKs and p38-MAPK (Fig. 3). MSK1 phosphorylation by H<sub>2</sub>O<sub>2</sub> was significantly reduced by ERK and p38-MAPK inhibitors as well as by inhibition of ERK upstream molecules, Src kinase and EGFR. The phosphorylation pattern of MSK1 followed closely the activation pattern of MAPKs. When both ERK and p38-MAPK were inhibited, we did not observe further inhibition of MSK1 phosphorylation. This may seem inconsistent, but we should take into consideration that it is unclear how the kinetics of ERK and p38-MAPK phosphorylation interact and coordinate MSK1 activation and that SB203580 can inhibit only the alpha and beta isoforms of p38-MAPK [53], while in skeletal muscle p38 gamma is largely expressed and may contribute to MSK1 phosphorylation as well. MSK1 phosphorylation by oxidative stress has been also reported in other cell types [54,55], although in those cases MSK1 activation was mediated only by p38-MAPK, and not by ERK. The activation of the kinase in the above studies was correlated with the subsequent activation of transcription factors (CREB and AP1, respectively).

As the transcription factor NF-κB is subjected to a complicated redox regulation in a cell-type specific manner [29], we examined its activation during oxidative stress in skeletal myoblasts. We found a mild time- and dose-dependent activation of NF-κB, as it was demonstrated by the increase in its DNA-binding activity, assessed by EMSA (Fig. 4). We also observed an increase in IκB phosphorylation (Ser32/36) by H<sub>2</sub>O<sub>2</sub>, exhibiting a similar profile with the DNA-binding activity of NF-κB (Fig. 5). However, we did not observe any decrease in IκB total levels, a result indicating that there is not

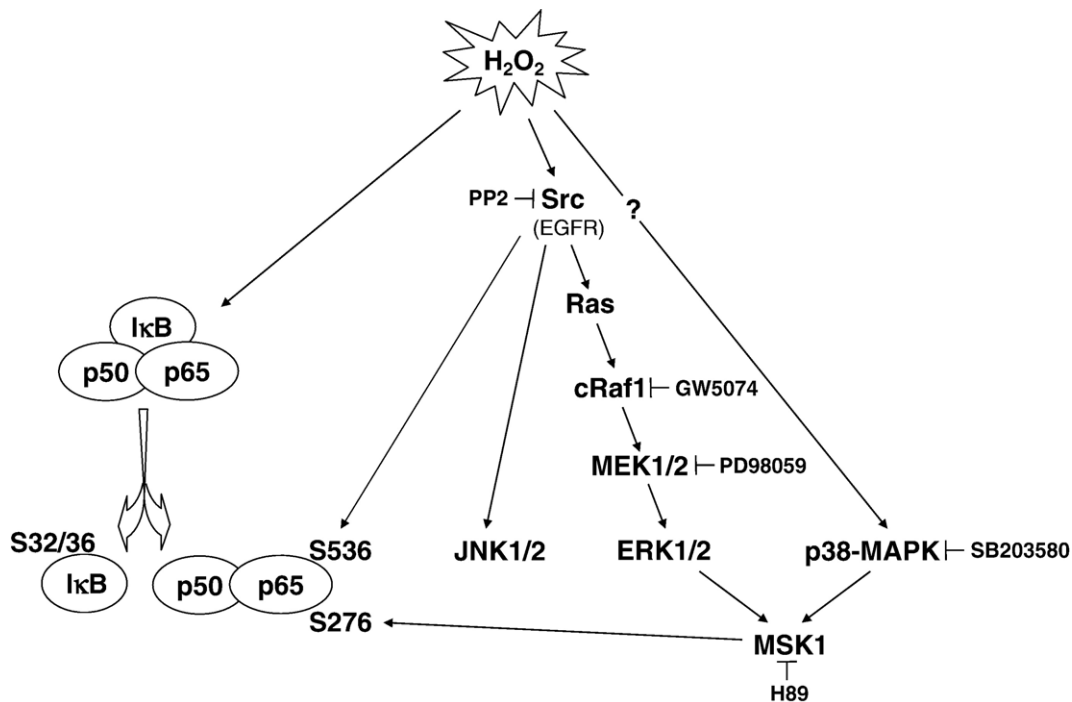


Fig. 11. A schematic model summarizing the results of this study. → induction, ⊖ inhibition.

any apparent degradation of I $\kappa$ B during oxidative stimulus. This result implies that there is an alternative activation mechanism of the transcription factor during this treatment. It has been reported that certain agents, including H<sub>2</sub>O<sub>2</sub>, activate NF- $\kappa$ B not through serine but through tyrosine phosphorylation of I $\kappa$ B and this may not lead to I $\kappa$ B degradation [56]. Thus, I $\kappa$ B remains bound to the dimer in the cytosol and only a small fraction of the transcription factor translocates into the nucleus. In other studies, another mechanism of NF- $\kappa$ B activation has been proposed, without the implication of I $\kappa$ B degradation, nor its tyrosine phosphorylation. This mechanism is based on reduced binding of NF- $\kappa$ B to I $\kappa$ B due to increased phosphorylation of p65 subunit of NF- $\kappa$ B [36]. These theories could explain the mild activation of NF- $\kappa$ B by H<sub>2</sub>O<sub>2</sub>, compared to the strong one observed during treatment with its potent inducer, TNF- $\alpha$ . Activation of NF- $\kappa$ B by oxidative stress has been previously reported in skeletal myotubes [57,58], correlated with their resistance to oxidative injury. The precise mechanism of NF- $\kappa$ B activation, however, was not examined in these studies. Zhou et al. [57] used a mutant I $\kappa$ B- $\alpha$  to inhibit NF- $\kappa$ B activation. This mutation involves the phosphorylation site of I $\kappa$ B. Thus, we may assume that the phosphorylation of I $\kappa$ B is important for NF- $\kappa$ B activation, even if it does not lead to I $\kappa$ B degradation.

A growing body of evidence supports that post-translational modifications play particularly important roles in the activation of NF- $\kappa$ B. Both phosphorylation and acetylation of p65 subunit of the transcription factor seem to be critical for the effective regulation of gene transcription by NF- $\kappa$ B. These modifications alter the ability of NF- $\kappa$ B dimers to bind DNA, recruit co-activators and bind I $\kappa$ B [33,59]. Recently, the transactivation of NF- $\kappa$ B has been linked with the MAPK substrates RSK1 and MSK1 that were shown to phosphorylate p65 subunit at serine 276 and serine 536, respectively [35,36]. To further investigate oxidative stress-mediated activation of NF- $\kappa$ B, we examined the phosphorylation status of these two residues, during H<sub>2</sub>O<sub>2</sub> treatment. As it is shown in Fig. 7, these two sites are phosphorylated by H<sub>2</sub>O<sub>2</sub>, in a time- and dose-dependent manner. The phosphorylation pattern of Ser276 is similar with that of MAPK and MSK1. On the contrary, the phosphorylation pattern of Ser536 is completely different compared to that of MAPK. Overall, it seems that the translocation of NF- $\kappa$ B dimer to the nucleus (as shown by EMSA) is accompanied with its phosphorylation at both aminoacid residues examined.

We further investigated whether MAPK pathways are implicated in any level of NF- $\kappa$ B activation. Using specific inhibitors of the kinases, we found that none of the MAPK pathways examined had an effect on H<sub>2</sub>O<sub>2</sub>-induced DNA binding activity of NF- $\kappa$ B or on Ser32/36 phosphorylation of I $\kappa$ B (Fig. 6). These results suggest that MAPKs are not involved in the processes leading to dissociation of NF- $\kappa$ B dimer from I $\kappa$ B and to nuclear translocation of the transcription factor.

Phosphorylation of p65 residue Ser536 was shown to be dependent on the Src kinase, while MAPKs were not implicated in this phosphorylation (Fig. 8). A kinase that has often been implicated in this phosphorylation is IKK, as has been shown during TNF- $\alpha$  treatment [59,60]. It is not known whether this is also the case during oxidative stimulus. An interesting point,

according to our data, is that Src kinase seems to mediate the activation of multiple, diverse signalling pathways during H<sub>2</sub>O<sub>2</sub> treatment.

On the other hand, our experiments showed that the phosphorylation of the other residue (Ser276) examined was mediated by MAPKs. In particular, we found that the inhibitors of p38-MAPK and ERKs, as well as the inhibitors of molecules upstream of ERKs (Src kinase and EGFR) reduced the H<sub>2</sub>O<sub>2</sub>-mediated phosphorylation of p65 at Ser276 (Fig. 9). Moreover, the potent inhibitor of MSK1, H89, diminished this phosphorylation. These results suggest that Ser276 of p65 could be a target for MSK1 during oxidative stimulus. This specific site is also phosphorylated by protein kinase A (PKA), during LPS (lipopolysaccharide) treatment [61] and H89 inhibits PKA as well. However, the fact that Ser276 phosphorylation is attenuated by inhibition of ERK and p38-MAPK, two kinases that have been shown to activate MSK1, further enhances the idea that this specific phosphorylation is mediated by MSK1. Still, whether MSK1 is the only Ser276-p65 kinase is uncertain.

## 5. Conclusions

Taken together, our results (summarized in Fig. 11) demonstrate that both MAPK and NF- $\kappa$ B pathways are activated during oxidative stress in skeletal myoblasts, providing evidence on their activation mechanisms. We show for the first time that MAPKs, in particular ERKs and p38-MAPK, are implicated in NF- $\kappa$ B transactivation by oxidative stimulus, and that this action is probably mediated by MSK1.

Overall, the regulation mechanisms involved in NF- $\kappa$ B activation are complicated; integrated signals arising from diverse pathways are required for its translocation and/or transactivation, reflecting the differential cell-type-dependent responses observed under oxidative stress.

## Acknowledgments

This work was funded by a GSRT grant (PENED 01 ED5).

## References

- [1] K.J. Davies, A.T. Quintanilha, G.A. Brooks, L. Packer, *Biochem. Biophys. Res. Commun.* 107 (1982) 1198.
- [2] M.J. Jackson, R.H. Edwards, M.C. Symons, *Biochim. Biophys. Acta* 847 (1985) 185.
- [3] F. McArdle, D.M. Pattwell, A. Vasilaki, A. McArdle, M.J. Jackson, *Free Radic. Biol. Med.* 39 (2005) 651.
- [4] M. Jackson, in: A.Z. Reznick, L. Packer, C.K. Sen, J.O. Holloszy, M.J. Jackson (Eds.), *Oxidative Stress in Skeletal Muscle, Free Radical Mechanisms in Exercise-related Muscle Damage*, Birkhauser Verlag, Basel, 1998, p. 75.
- [5] T.A. Rando, *Am. J. Phys. Med. Rehabil.* 81 (2002) S175.
- [6] H. Kondo, I. Nakagaki, S. Sasaki, S. Hori, Y. Itokawa, *Am. J. Physiol.: Endocrinol. Metab.* 265 (1993) E839.
- [7] S.K. Powers, A.N. Kavazis, K.C. DeRuisseau, *Am. J. Physiol., Regul. Integr. Comp. Physiol.* 288 (2005) R337.
- [8] A. McArdle, J.H. van der Meulen, M. Catapano, M.C.R. Symons, J.A. Faulkner, M.J. Jackson, *Free Radic. Biol. Med.* 26 (1999) 1085.
- [9] V. Adler, Z. Yin, K.D. Tew, Z. Ronai, *Oncogene* 18 (1999) 6104.
- [10] J.J. Haddad, *Cell. Signal.* 14 (2002) 879.

- [11] Y. Sun, L.W. Oberley, *Free Radic. Biol. Med.* 21 (1996) 335.
- [12] W. Droge, *Physiol. Rev.* 82 (2002) 47.
- [13] C. Widmann, S. Gibson, M.B. Jarpe, G.L. Johnson, *Physiol. Rev.* 79 (1999) 143.
- [14] J.M. Kyriakis, J. Avruch, *Physiol. Rev.* 81 (2001) 807.
- [15] S. Ghosh, M. Karin, *Cell* 109 (2002) S81.
- [16] G. Pearson, F. Robinson, T. Beers Gibson, B.E. Xu, M. Karandikar, K. Berman, M.H. Cobb, *Endocr. Rev.* 22 (2001) 153.
- [17] P.P. Roux, J. Blenis, *Microbiol. Mol. Biol. Rev.* 68 (2004) 320.
- [18] J.I. Abe, B.C. Berk, *J. Biol. Chem.* 274 (1999) 21003.
- [19] M. Yoshizumi, J. Abe, J. Haendeler, Q. Huang, B.C. Berk, *J. Biol. Chem.* 275 (2000) 11706.
- [20] K. Chen, J.A. Vita, B.C. Berk, J.F. Keaney Jr., *J. Biol. Chem.* 276 (2001) 16045.
- [21] S. Zhongang, R.G. Schnellmann, *Am. J. Physiol., Renal Fluid Electrolyte Physiol.* 286 (2004) F858.
- [22] S. Purdom, Q.M. Chen, *J. Pharmacol. Exp. Ther.* 312 (2005) 1179.
- [23] J. Matsukawa, A. Matsuzawa, K. Takeda, H. Ichijo, *J. Biochem. (Tokyo)* 136 (2004) 261.
- [24] W. Zhang, S. Zheng, P. Storz, W. Min, *J. Biol. Chem.* 280 (2005) 19036.
- [25] H. Ichijo, E. Nishida, K. Irie, P. ten Dijke, M. Saitoh, T. Moriguchi, M. Takagi, K. Matsumoto, K. Miyazono, Y. Gotoh, *Science* 275 (1997) 90.
- [26] M. Saitoh, H. Nishitoh, M. Fujii, K. Takeda, K. Tobiume, Y. Sawada, M. Kawabata, K. Miyazono, H. Ichijo, *EMBO J.* 17 (1998) 2596.
- [27] N.K. Tonks, *Cell* 121 (2005) 667.
- [28] R. Schreck, P.A. Baeuerle, *Trends Cell Biol.* 1 (1991) 39.
- [29] N. Li, M. Karin, *FASEB J.* 13 (1999) 1137.
- [30] S. Ghosh, M.J. May, E.B. Kopp, *Annu. Rev. Immunol.* 16 (1998) 225.
- [31] M. Karin, Y. Ben-Neriah, *Annu. Rev. Immunol.* 18 (2000) 621.
- [32] M.L. Schmitz, S. Bacher, M. Kracht, *Trends Biochem. Sci.* 26 (2001) 186.
- [33] L. Vermeulen, G. De Wilde, S. Notebaert, W. Vanden Berghe, G. Haegeman, *Biochem. Pharmacol.* 64 (2002) 963.
- [34] L.F. Chen, W.C. Greene, *Nat. Rev., Mol. Cell Biol.* 5 (2004) 392.
- [35] L. Vermeulen, G. De Wilde, P. Van Damme, W. Vanden Berghe, G. Haegeman, *EMBO J.* 22 (2003) 1313.
- [36] J. Bohuslav, L.F. Chen, H. Kwon, Y. Mu, W.C. Greene, *J. Biol. Chem.* 279 (2004) 26115.
- [37] W. Vanden Berghe, S. Plaisance, E. Boone, K. De Bosscher, M.L. Schmitz, W. Fiers, G. Haegeman, *J. Biol. Chem.* 273 (1998) 3285.
- [38] R. Craig, A. Larkin, A.M. Mingo, D.J. Thuerauf, C. Andrews, P.M. McDonough, C.C. Glembofski, *J. Biol. Chem.* 275 (2000) 23814.
- [39] B. Baeza-Raja, P. Munoz-Canoves, *Mol. Biol. Cell* 15 (2004) 2013.
- [40] T.J. Hawke, D.J. Garry, *J. Appl. Physiol.* 91 (2001) 534.
- [41] D. Yaffe, O. Saxel, *Nature* 270 (1977) 725.
- [42] E. Schreiber, P. Matthias, M.M. Muller, W. Schaffner, *Nucleic Acids Res.* 17 (1989) 6419.
- [43] T. Markou, M. Hadzopoulou-Cladaras, A. Lazou, *J. Mol. Cell. Cardiol.* 37 (2004) 1001.
- [44] T. Mosmann, *J. Immunol. Methods* 65 (1983) 55.
- [45] H.N. Nguyen, C. Wang, D.C. Perry, *Brain Res.* 924 (2002) 159.
- [46] S. Thomson, A.L. Clayton, C.A. Hazzalin, S. Rose, M.J. Barratt, L.C. Mahadevan, *EMBO J.* 18 (1999) 4779.
- [47] T.A. Rando, M.H. Disatnik, Y. Yu, A. Franco, *Neuromuscul. Disord.* 8 (1998) 14.
- [48] S.T. Winokur, K. Barrett, J.H. Martin, J.R. Forrester, M. Simon, R. Tawil, S.A. Chung, P.S. Masny, D.A. Figlewicz, *Neuromuscul. Disord.* 13 (2003) 322.
- [49] J.C. Dai, P. He, X. Chen, E.M. Greenfield, *Bone* (2005), doi:10.1016/j.bone.2005.10.007.
- [50] S.C. Lien, S. Usami, S. Chien, J.J. Chiu, *Cell. Signal.* (2005), doi:10.1016/j.cellsig.2005.10.013.
- [51] P.A. Bromann, H. Korkaya, S.A. Courtneidge, *Oncogene* 23 (2004) 7957.
- [52] J.S. Biscardi, M.C. Maa, D.A. Tice, M.E. Cox, T.H. Leu, S.J. Parsons, *J. Biol. Chem.* 274 (1999) 8335.
- [53] S. Kumar, J. Boehm, J.C. Lee, *Nat. Rev. Drug Discov.* 2 (2003) 717.
- [54] M. Deak, A.D. Clifton, L.M. Lucocq, D.R. Alessi, *EMBO J.* 17 (1998) 4426.
- [55] I.K. Aggeli, C. Gaitanaki, I. Beis, *Cell. Signal.* (2006), doi:10.1016/j.cellsig.2006.02.001.
- [56] Y. Takada, A. Mukhopadhyay, G.C. Kundu, G.H. Mahabeleshwar, S. Singh, B.B. Aggarwal, *J. Biol. Chem.* 278 (2003) 24233.
- [57] L.Z. Zhou, A.P. Johnson, T.A. Rando, *Free Radic. Biol. Med.* 31 (2001) 1405.
- [58] M.V. Catani, I. Savini, G. Duranti, D. Caporossi, R. Ceci, S. Sabatini, L. Avigliano, *Free Radic. Biol. Med.* 37 (2004) 1024.
- [59] M.S. Hayden, S. Ghosh, *Genes Dev.* 18 (2004) 2195.
- [60] H. Sakurai, S. Suzuki, N. Kawasaki, H. Nakano, T. Okazaki, A. Chino, T. Doi, I. Saiki, *J. Biol. Chem.* 278 (2003) 36916.
- [61] H. Zhong, H. SuYang, H. Erdjument-Bromage, P. Tempst, S. Ghosh, *Cell* 89 (1997) 413.